Available online at www.sciencedirect.com
ScienceDirect
Chemical Physics 327 (2006) 269–277
Chemical Physics
www.elsevier.com/locate/chemphys

Electron momentum spectroscopy study of thiophene: Binding energy spectrum and valence orbital electron density distributions

S.F. Zhang [a,b], X.G. Ren [a,b], G.L. Su [a,b], C.G. Ning [a,b], H. Zhou [a,b], B. Li [a,b], G.Q. Li [a,b], J.K. Deng [a,b,*]

[a] Department of Physics, Tsinghua University, Beijing 100084, PR China
[b] Key Laboratory of Atomic and Molecular NanoSciences, MOE, PR China

Received 25 January 2005; accepted 2 May 2006
Available online 8 May 2006

Abstract

Electron momentum spectroscopy has been used to measure the binding energy spectrum and momentum distributions of the valence orbitals of thiophene, which are compared with Hartree–Fock and density functional theory calculations using different-sized basis sets. Impact energy of 1200 eV plus binding energy and symmetric non-coplanar kinematics are employed. The measured binding energy spectra are compared and consistent with PES data available in the literature and also with the predictions of Green's function methods. The agreement between theory and experiment for the shape of the orbital electron momentum distributions is generally good. The satellite structure of the innermost valence orbital $6a_1$ is reported.

Keywords: Electron momentum spectroscopy; Hartree–Fork; DFT; Basis set; Thiophene

1. Instruction

Electron momentum spectroscopy (EMS), which is a powerful and informative experimental tool for studying the electronic structure of atoms and molecules, can provide some significant information on electron motion and electron correlation. This information has lead to improve theoretical models for the electronic wavefunctions [1–4]. The results have also provided improved understanding of the relation between electron density distribution and chemical reactivity [5,6]. EMS can access the complete valence-shell binding energy range, though with lower resolution than that in most photoelectron spectroscopy (PES) studies, and the orbital electron density imaging information provided by EMS momentum profiles is unique. EMS measurements of the momentum profiles for individual orbitals in atoms and molecules have been shown to provide a sensitive method for the evaluation and design of accurate self-consistent field (SCF) and highly correlated molecular wavefunctions as well as density functional theory (DFT) methods. Such wavefunctions developed through interactive collaboration between quantum theory and EMS measurements have been found to be of an essentially "universal" nature in that they are suitable for quite accurate calculations of a wide range of properties, each emphasizing different regions of phase space. For example, total energies, dipole (or quadrupole) moments, and momentum profiles respectively emphasize small, medium, and large r regions [3,4].

The application of EMS to the study of the outermost orbitals in molecules has shown that the method is particularly sensitive to those aspects of the electronic structure that are most important in determining the chemical and physical properties of atoms and molecules. It provides an excellent test of ab initio calculations and indicates that it is important to include long range correlation effects [7]. In particular, the inner valence region of the binding energy

* Corresponding author.
E-mail address: djk-dmp@mail.tsinghua.edu.cn (J.K. Deng).

0301-0104/$ - see front matter © 2006 Elsevier B.V. All rights reserved.
doi:10.1016/j.chemphys.2006.05.002

spectrum provides a very sensitive test for many-body calculations that take both initial and final state correlation into account [8].

The five-membered aromatic heterocyclic molecules furan (C_4H_4O), pyrrole (C_4H_5N) and thiophene (C_4H_4S) have attracted a lot of attention because of important applications in many chemical areas such as organic synthesis, polymer production and pesticides manufacture [9–11]. The outer valence region of thiophene has been extensively studied experimentally by various methods: HeI and HeII PES [12–14], UV PES [15], X-ray PES [16,17], synchrotron radiation [9,18], Penning ionization electron spectroscopy, etc. Furan and pyrrole have been researched by EMS [19,20], but no EMS study of thiophene has been reported to the best of our knowledge.

2. Theoretical background and calculations details

The EMS reaction theory is based on several approximations, through which the binary (e, 2e) cross-section is related to the electronic structure of the target. Of these the most important are: (i) the binary encounter approximation, which assumes that the interaction operator depends only on the coordinates of the two outgoing electrons and not on those of the remaining particles constituting the ion, and (ii) the plane-wave impulse approximation (PWIA), in which the incident and both two outgoing electrons are represented by plane waves. In the PWIA, the momentum p of the electron prior to knock-out is related to the azimuthal angle ϕ by

$$p = [(2p_1 \cos\,\theta_1 - p_0)^2 + (2p_1 \sin\,\theta_1 \sin\,(\phi/2))^2]^{1/2} \tag{1}$$

where $p_1 = p_2 = \sqrt{2E_1}$ is the magnitude of the momentum of each outgoing electron and $p_0 = \sqrt{2E_0}$ is the momentum of the incident electron (both in atomic units).

In order to ensure the validity of these approximations the experiment has to be carried out under what are known as EMS conditions, which are sufficiently high electron impact energy (typically 1200 eV plus the binding energy) and large momentum transfer, optimally, the use of the symmetric non-coplanar kinematics. When these EMS conditions are met it has been shown that the kinematic factors are effectively constant and that the differential cross-section for (e, 2e) is then proportional to the spherically averaged momentum distribution of the corresponding Dyson orbital

$$\sigma_{\mathrm{EMS}} \propto \int \left|\langle p\Psi_{\mathrm{f}}^{N-1}\left|\Psi_0^N\right\rangle\right|^2 \mathrm{d}\Omega \tag{2}$$

where $\int \mathrm{d}\Omega$ denotes spherical averaging over the full solid angle to account for the random orientation of gaseous target molecules and p is a plane wave spin orbital for an electron momentum. The Dyson orbital is given explicitly by the overlap of the N-electron wavefunction describing the initial state and the $(N-1)$-electron wavefunction describing the final ion state. The Dyson orbitals can be evaluated using the configuration interaction (CI) and Green function (GF), or be further approximated by the corresponding canonical Hartree–Fock (HF) orbitals, and this then gives the target Hartree–Fock approximation (THFA) in which

$$\sigma_{\mathrm{EMS}} \propto S_{\mathrm{j}}^{\mathrm{f}} \int \mathrm{d}\Omega \left|\psi_{\mathrm{j}}^{\mathrm{HF}}(p)\right|^2 \tag{3}$$

Alternatively, σ_{EMS} may be evaluated by DFT using canonical Kohn–Sham orbitals to approximate the Dyson orbitals and this gives the target Kohn–Sham approximation (TKSA)

$$\sigma_{\mathrm{EMS}} \propto S_{\mathrm{j}}^{\mathrm{f}} \int \mathrm{d}\Omega \left|\psi_{\mathrm{j}}^{\mathrm{KS}}(p)\right|^2 \tag{4}$$

In Eqs. (3) and (4), $\psi_{\mathrm{j}}^{\mathrm{HF}}(p)$ and $\psi_{\mathrm{j}}^{\mathrm{KS}}(p)$ are the respective momentum space representations of the corresponding canonical HF or canonical Kohn–Sham orbital (j) from which the electron was ionized. It should be noted that the DFT TKSA description takes the initial state electron correlation effects through the exchange–correlation into account. The quantity $S_{\mathrm{j}}^{\mathrm{f}}$ in Eqs. (3) and (4) is the spectroscopic factor [21] or pole strength and also is the probability of the ionization event producing a $(\psi_{\mathrm{j}})^{-1}$ one-hole configration of the final ion state, $|\Psi_{\mathrm{f}}^{\mathrm{N\text{-}1}}\rangle$. This factor can arise from final state electron correlation and relaxation effects [22].

In the present work, spherically averaged theoretical momentum profiles have been calculated for the all valence orbitals of thiophene using the PWIA. The calculations methods and basis sets are described briefly below and in Table 1. The total number of contracted Gaussian-type orbital functions (CGTO) is also given for each calculation below. The total energies and the dipole moments of thiophene predicted by these various calculations and the experimental dipole moment [23] are also listed in Table 1. An effective quantum mechanical description in all regions of phase space should provide good values of total energy, dipole moment and the momentum distributions, properties which have short r (large p), medium r (medium p), and large r (low p) emphases, respectively [3,4].

The calculations of thiophene have been carried out at the ab initio level in the present work. The geometry of thiophene [17–19] has been used for all the calculations. Details of the calculation methods are described below. The Hartree–Fock and DFT calculations were carried out using the GAUSSIAN 98W program together with the MOMAP program developed by UBC. In order to compare the calculated cross-sections with the experimental electron momentum profiles, the effects of the finite spectrometer acceptance angles in both θ and ϕ ($\Delta\theta = \pm 0.6°$ and $\Delta\phi = \pm 1.2°$) were included using the Gaussian-weighted planar grid (GW-PG) method [24] performed by the Resfold program. The HF calculations of the momentum profiles were performed by using Eq. (3) with the basis sets of STO-3G, 6-31G, 6-311++G (3df, 3pd) and aug-cc-pVTZ. The B3LYP [25] hybrid functional is used for the DFT calculations, respectively, and with three basis sets of 6-31G, 6-311++G (3df, 3pd) and aug-cc-pVTZ.

Table 1
Basis sets and calculated properties for thiophene

Calculation method and basis set	Contracted Gaussian basis set [S]/[C]/[H]	Total energy (a.u.)	Dipole moment[a] (Debye)
HF/STO-3G	[3s,2p]/[2s,1p]/[1s]	−545.0886272	0.2503
HF/6-31G	[4s,3p]/[3s,2p]/[2s]	−551.1842115	1.0514
HF/6-311++G (3df, 3pd)	[7s,6p,3d,1f]/[5s,4p,3d,1f]/[4s,3p,1d]	−551.3746798	0.6371
HF/aug-cc-pVTZ	[6s,5p,3d,2f]/[5s,4p,3d,2f]/[4s,3p,2d]	−551.3813982	0.6597
DFT/B3LYP/6-31G	[4s,3p]/[3s,2p]/[2s]	−552.9250780	0.7509
DFT/B3LYP/6-311++G (3df, 3pd)	[7s,6p,3d,1f]/[5s,4p,3d,1f]/[4s,3p,1d]	−553.0992814	0.4694
DFT/B3LYP/ aug-cc-pVTZ	[6s,5p,3d,2f]/[5s,4p,3d,2f]/[4s,3p,2d]	−553.1053708	0.4799
Experiment [40]			0.550

[a] For non-rotating, non-vibrating molecule at equilibrium internuclear spacings.

(1) *STO-3G*: A standard minimal basis set, effectively of single zeta quality, using a single contraction of three Gaussian functions for each basis functions. A total of 33 CGTO is employed for thiophene. This basis set was designed by Pople and co-workers [26,27].
(2) *6-31G*: This is a split valence basis set and it comprises an inner valence shell of six s-type Gaussians and an outer valence shell, which has been split into two parts represented by three and one primitives. For thiophene this is a 57-CGTO basis. A detailed description of this basis set developed by Pople and the co-workers can be found in Refs. [28,29].
(3) *6-311++G (3df, 3pd)*: The 6-311++G (3df, 3pd) is an augmented version by Pople et al. [30]. The outer valence shell is split into three parts and represented by three, one and one primitives, respectively. 6-311++G (3df, 3pd) designates the 6-311G basis set supplemented by diffuse functions on both heavy atoms and hydrogen atom, three sets of d-functions and one set of f-functions on heavy atoms, and supplemented by three sets of p-functions and one set of d-functions on hydrogens. It is significant valuable to describe the electron correlation effect. The number of CGTO is 275 for thiophene.
(4) *aug-cc-pVTZ*: It is the abbreviation for the augmented correlation consistent polarized valence triple-zeta basis set developed by Dunning and his co-workers [31,32]. This large basis set description adds both polarization and diffuse functions to an already triple-zeta description of the thiophene valence orbitals. The Hatree–Fock calculations were performed with a spherical harmonic basis set to avoid linear dependence problems in the d and f functions. The basic idea behind the correlation consistent basis sets is that functions which contribute approximately the same amount of correlation energy should be grouped together when considering what mixture of s, p, d, etc. basis functions to use. The aug-cc-pVTZ basis places one s, one d, and one p diffuse functions on hydrogen atoms, and one s, one p, one d, and one f diffuse functions on B through Ne and Al through Ar. This is a 326-CGTO basis for thiophene.

3. Experimental apparatus

A detailed description of the EMS spectrometer in this work has been given elsewhere [33]. In brief, gaseous target atoms or molecules are ionized by impact with a well focused electron beam of defined energy (1200 eV plus binding energy). Both outgoing electrons (scattered and ejected) are energy selected and detected in coincidence. The present experiment has been performed in the symmetric non-coplanar geometry, i.e. both outgoing electrons are detected at equal energies $E_1 = E_2 = 600$ eV and equal polar angles $\theta_1 = \theta_2 = 45°$. The relative azimuthal angle ϕ is variable.

In present EMS measurements, the individual orbitals are selected by the choice of the binding energy. In order to obtain the experimental momentum profiles corresponding to the main peaks in the outer and inner valence regions with the multi-channel energy dispersive spectrometer, wide range binding energy spectra (BES) are collected at a series of azimuthal (out of plane) angles ϕ over the range of 0° to ±30° in a series of sequential repetitive scans.

Momentum distributions as a function of angle ϕ are obtained by deconvolution of these binding energy spectra using Gaussian functions located at the each ionization energy in the BES. The widths and relative position of the Gaussian functions can be determined from a consideration of published high resolution PES vibronic manifolds and the EMS instrumental energy resolution function (1.2 eV FWHM). For each ionization process, the area of the fitted peak (or the integral of the spectral region, where appropriate) is plotted as a function of momentum calculated from ϕ using Eq. (1). A given set of areas as a function of momentum for a specific binding energy is referred to as an experimental momentum profile (XMP). To compare the XMPs with the relative cross-sections calculated as a function of momentum using expressions (2) and (3) above, the effects of the finite spectrometer acceptance angles in both θ and ϕ ($\Delta\theta = \pm 0.6°$ and $\Delta\phi = \pm 1.2°$) were included in the calculations. This is achieved in the present work by using the GW-PG method [24]. After momentum resolution folding, the calculation (Eqs. (2), (3) or (4)) is referred to as a theoretical momentum profile (TMP).

All multichannel measurements in the present work were obtained using the "binning" mode [4]. The sample

of thiophene (⩾98.0% purity) was used without further purification other than freeze–thaw cycles which used to remove dissolved air. No impurities were observed in any of the binding energy spectra.

4. Result and discussion

The point group symmetry of thiophene is C_{2v}. According to molecular orbital theory, the ground state electronic configuration can be written as

$$(\text{core})^{18}\underbrace{(6a_1)^2(4b_2)^2(7a_1)^2}_{\text{inner valence}}\underbrace{(8a_1)^2(5b_2)^2(9a_1)^2(6b_2)^2(10a_1)^2(7b_2)^2(2b_1)^2(11a_1)^2(3b_1)^2(1a_2)^2}_{\text{outer valence}}$$

In the ground state, the 44 electrons are arranged in 22 double-occupied orbitals in the independent particle description. The valence electrons in thiophene are distributed in 13 molecular orbitals. All the canonical molecular orbitals are either a-type or b-type. There is no degeneracy in these orbitals therefore the spectra of thiophene are not complicated by the Jahn–Teller effect.

4.1. Binding energy spectrum

The ionization potentials measured by PES [12,18] and present EMS, as well as the HF and DFT orbital energies for the outer valence orbitals, are shown in Table 2. In addition, an outer-valence-shell Green's function (OVGF) [34] calculation of ionization potentials (IPs) and pole strength for outer valence orbitals of thiophene has also been performed with the 6-311++G** basis set. In the PES work [12], the vertical IPs of the $1a_2$, $3b_1$, $11a_1$, $2b_1$, $7b_2$, $10a_1$, $6b_2$, $9a_1$, $5b_2$ and $8a_1$ orbitals were determined to be 8.87, 9.52, 12.1, 12.7, 13.3, ~13.9, 14.3, 16.6, 17.6 and ~18.3 eV, respectively.

Calculated binding energy spectrum is compared with the measured binding energy spectrum in Fig. 1. The synthesized theoretical spectrum is obtained by summing the calculated densities over the same momentum range as the experiment, and using the calculated energy levels of the different orbitals. Both of the calculated density and energy levels of different orbitals come from the DFT-B3LYP/aug-cc-pVTZ calculation. In comparing the experimental and theoretical binding energy spectrum, it should be noted that the calculated energy levels has been shifted by 2.1 eV so that the average energy of the $(9a_1 + 5b_2)$ orbitals agrees with the corresponding 16.6 eV peak in the experimental PES. The theoretical spectrum is height normalized to the summed experimental spectrum on the $(9a_1 + 5b_2)$ peak. The same overall energy widths used for the Gaussian fits of the experimental spectra have been folded into the calculated spectrum.

In the EMS binding energy spectra of Fig. 2, however, only eight structures can be clearly identified. In the regions, where there are two or more peaks overlapping within an energy separation of the order of 1.0 eV or less, it is not possible to separate their individual contributions with the present EMS energy resolution of 1.2 eV. The average vertical IPs of the $(1a_2 + 3b_1)$, $(11a_1 + 2b_1 + 7b_2 + 10a_1 + 6b_2)$, $(9a_1 + 5b_2)$, and $8a_1$ outer orbitals are determined by the present EMS measurement to be 9.2, 12.9, 16.6 and 18.4 eV, respectively. The differences in FWHM are due to the vibrational broadening of the lines. The binding energy values in Fig. 2 are similar to the IPs in the PES obtained by Von Niessen et al. [12].

It can be seen from Fig. 1 that the DFT-B3LYP/aug-cc-pVTZ calculation is in reasonably good agreement with the experimental binding energy spectra for both relative energy position and intensity in the outer valence region (below 20 eV). However, the calculation predicted significant splitting of ionization transitions from the $6a_1$ orbital due to strong electron correlation effects in the inner

Table 2
Outer valence ionization potentials for thiophene (eV)

Orbital	Experiment			OVGF[c]		Orbital energy	
	EMS	PES[a]	PES[b]	Ionization potential	Pole strength	HF[d]	DFT[e]
$1a_2$	9.2	9.0	8.87	8.834	0.901	−8.926	−6.633
$3b_1$		9.5	9.52	9.065	0.906	−9.419	−7.022
$11a_1$	12.9	12.0	12.1	11.983	0.900	−12.912	−9.474
$2b_1$		12.5	12.7	12.824	0.826	−14.251	−10.498
$7b_2$		13.2	13.3	13.312	0.901	−14.397	−10.671
$10a_1$		13.9	~13.9	13.354	0.896	−14.971	−10.800
$6b_2$		14.4	14.3	14.126	0.893	−15.698	−11.355
$9a_1$	16.6	16.6	16.6	17.114	0.854	−19.010	−14.155
$5b_2$		17.6	17.6	18.347	0.845	−20.464	−15.158
$8a_1$	18.4	18.4	~18.3	19.019	0.047	−20.859	−15.423

[a] From Ref. [18]
[b] From Ref. [12]
[c] This work, calculated by OVGF method and the 6-311++G** basis set.
[d] This work, calculated by HF method and the aug-cc-pVTZ basis set.
[e] This work, calculated by DFT/B3LYP method and the aug-cc-pVTZ basis set.

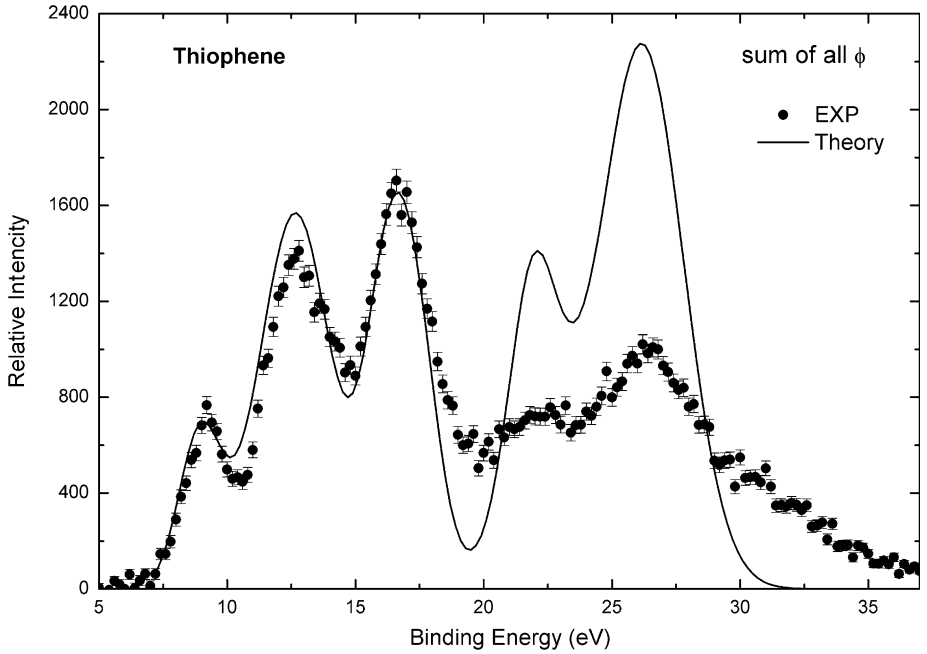

Fig. 1. Experimental and synthetic binding energy spectra of thiophene at sum of all ϕ angles. The solid curve is the DFT-B3LYP calculation with aug-cc-pVTZ basis set. See text for details.

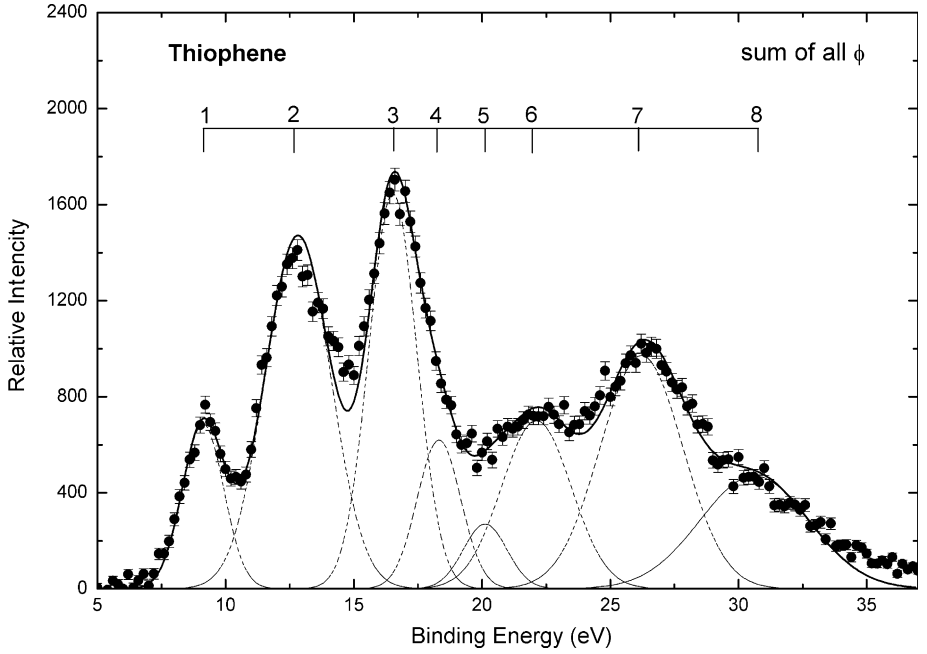

Fig. 2. Valence shell binding energy spectrum of 1200 eV for thiophene (sum of all ϕ). The dashed and solid curves represent individual and summed Gaussian fits, respectively. The position of individual transitions determined by high-resolution PES are shown as bars with numbers 1–8, which correspond to $(1a_2 + 3b_1)$, $(11a_1 + 2b_1 + 7b_2 + 10a_1 + 6b_2)$, $(9a_1 + 5b_2)$, $8a_1$, $7a_1$, $4b_2$, $6a_1$ ionization and the satellite band, respectively.

valence region. The calculation underestimates the intensity of the ionization transition above 30 eV, which suggests that the theory should contain lower pole strength for the $6a_1$ orbital and this is also consistent with the comparison of the measured and calculated momentum profiles of the $6a_1$ orbital presented in the following subsection.

4.2. Comparison of experimental and theoretical momentum profiles

The experimental momentum profiles are extracted by deconvolving the same peak from the sequentially obtained binding energy spectra at different azimuthal angles or

momentum [1,2,7]. In order to compare the experimental momentum distributions with the theoretical ones, we need one normalization factor common for all bands. Usually, this normalization factor is determined by normalizing the experimental and theoretical momentum distributions of the outermost valence ionization to the common intensity scale, since the outermost valence ionizations are expected to exhibit pole strength close to unity. In this work, the observed band areas in the outer valence between 5 and 20 eV at all measured ϕ have been summed up, and then normalized to the sum of the TMPs of the outer valence orbitals calculated using the DFT-B3LYP method and the aug-cc-pVTZ basis set. The relative normalization is preserved for all other orbitals in Figs. 3–9.

Fig. 3 shows the XMP for the summed ($1a_2 + 3b_1$) frontier orbitals of thiophene. Although they are not experimentally separated due to the close energy spacing (see the above discussion), individual TMPs have been calculated using the HF and DFT methods and are shown in the figure. The HOMO $1a_2$ and NHOMO $3b_1$ are π molecular orbitals (denoted π_2, π_3), which are mainly due to the p-electrons donated by the carbon atoms together with the lone-pair from the sulfur atom, and thus they have a "p-type" momentum distributions. In order to make the TMPs and XMP agree with each other, it is necessary to multiply the TMPs by a factor of 0.90. Thus, the pole strengths S_j^f of the $1a_2^{-1}$ and $3b_1^{-1}$ states are determined to be 0.90. These are in good agreement with the theoretical pole strength of 0.92 by Von Niessen et al. [12]. Some discrepancies between the TMPs and XMP in the low momentum region can be attributed to the error limits of the data.

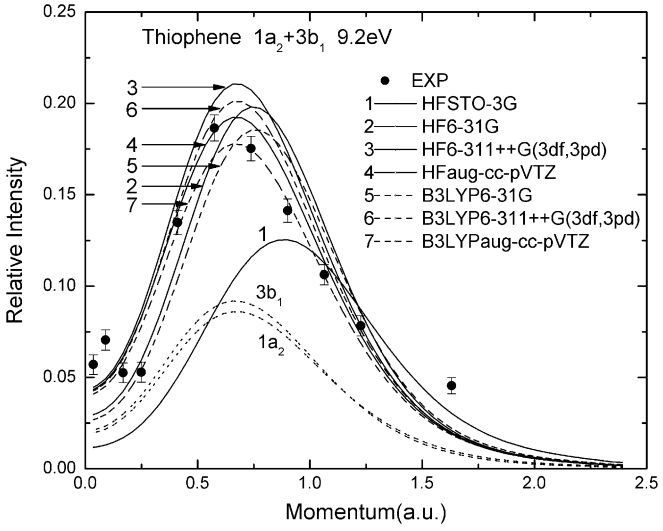

Fig. 3. Experimental and calculated momentum distributions for the HOMO and NHOMO summed orbitals ($1a_2$+$3b_1$) of thiophene. The summed TMPs are calculated by using Hartree–Fock (curves 1–4) with the STO-3G, 6-31G, 6-311++G (3df, 3pd) and aug-cc-pVTZ basis sets and DFT-B3LYP (curves 4–7) methods with the 6-31G, 6-311++G (3df, 3pd) and aug-cc-pVTZ basis sets. The individual theoretical momentum distributions of the HOMO and NHOMO, obtained using the DFT-B3LYP method with the aug-cc-pVTZ basis set, are shown by dotted curves. All of the TMPs are scaled by a factor of 0.90.

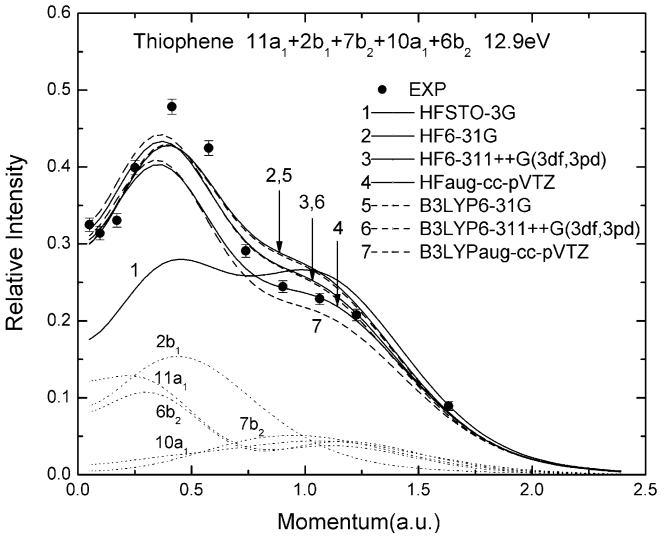

Fig. 4. Experimental and calculated momentum distributions for the summed and individual orbitals of $11a_1$, $2b_1$, $7b_2$, $10a_1$ and $6b_2$ of thiophene. The calculations of the summed TMPs are similar to above. The individual theoretical momentum distributions of the five orbitals obtained using the DFT-B3LYP method with the aug-cc-pVTZ basis set are shown by dotted curves.

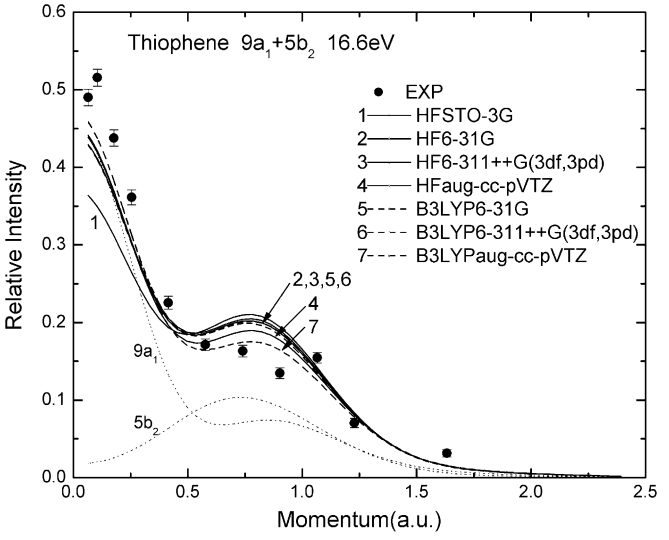

Fig. 5. Experimental and calculated momentum distributions for the summed and individual orbitals of $9a_1$ and $5b_2$ of thiophene. The calculations of the summed TMPs are similar to above. The individual theoretical momentum distributions of the $9a_1$ and $5b_2$ orbitals obtained using the DFT-B3LYP method with the aug-cc-pVTZ basis set are shown by dotted curves.

The application of EMS to the study of the outermost orbitals in molecules has shown that the method is particularly sensitive to those aspects of the electronic structure that are most important in determining the chemical and physical properties of atoms and molecules. It provides an excellent test of ab initio calculations and indicates when it is important to include long range correlation effects. It can be seen that the HF calculation with STO-3G minimal basis set (curve 1 in Fig. 3) does not give a well

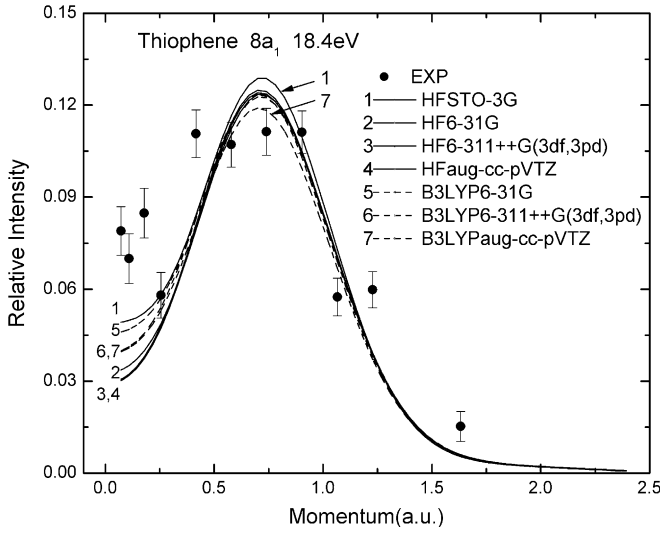

Fig. 6. Experimental and calculated momentum distributions for the $8a_1$ orbital of thiophene. The calculations of the TMPs are similar to above.

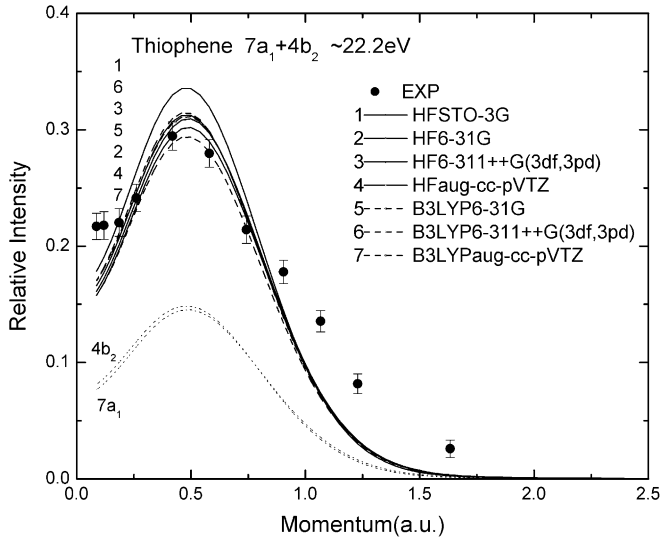

Fig. 7. Experimental and calculated momentum distributions for the summed and individual orbitals of $7a_1$ and $4b_2$ of thiophene. The calculations of the summed TMPs are similar to above. The individual theoretical momentum distributions of the $7a_1$ and $4b_2$ orbitals obtained using the DFT-B3LYP method with the aug-cc-pVTZ basis set are shown by dotted curves.

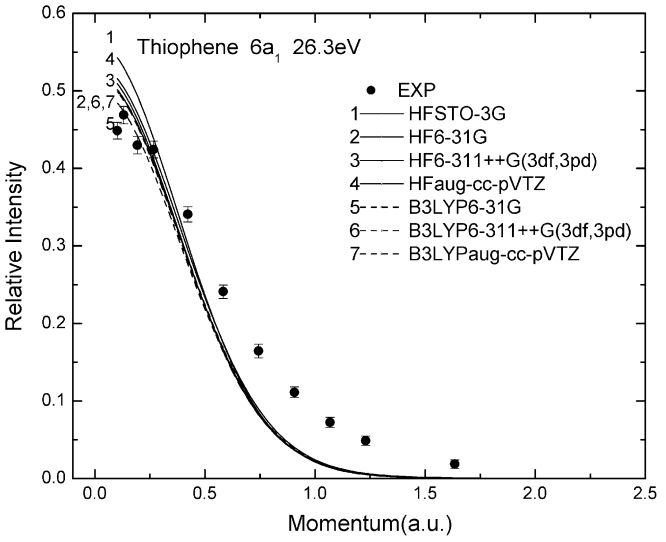

Fig. 8. Experimental and calculated momentum distributions for the $6a_1$ orbital of thiophene. The calculations of the TMPs are similar to above. All calculations have been multiplied by a factor of 0.60.

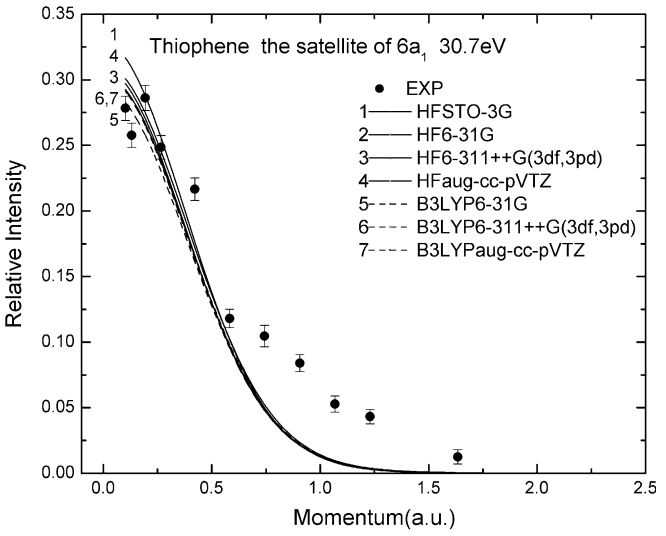

Fig. 9. Experimental and calculated momentum distributions for the satellite of $6a_1$ orbital of thiophene. The calculations of the TMPs are similar to above. All calculations have been multiplied by a factor of 0.35.

description to the XMP. The HF and DFT-B3LYP calculations with 6-311++G (3df, 3pd) basis set (curves 3 and 6) give the accurate position of the maximum intensity ($p_{max} \approx 0.65$ a.u.) but overestimate the measured intensity. However, the HF and DFT-B3LYP calculations with aug-cc-pVTZ basis set (curves 4 and 7) give both the proper intensity in whole momentum region and the accurate position of the maximum intensity. For 6-311++G (3df, 3pd) basis set, the DFT-B3LYP calculations give the better description to the XMP than the HF calculations, and so does the aug-cc-pVTZ basis set. This indicates that inclusion of dynamic electron correlation effects is essential for modeling the chemically important larger r (lower p) region of the frontier orbitals ($1a_2 + 3b_1$) of thiophene.

The second peak at 12.9 eV in the binding energy spectrum in Fig. 2 is associated with the ionizations of the $11a_1$, $2b_1$, $7b_2$, $10a_1$ and $6b_2$ orbitals. These orbitals are not well separated experimentally due to their small energy separations. Therefore, the summed momentum distributions of the $11a_1$, $2b_1$, $7b_2$, $10a_1$ and $6b_2$ orbitals are discussed for comparison between experiment and theory. Fig. 4 shows that the summed XMPs have a "p-ptype" distribution. The comparison of the summed XMPs with various calculations in Fig. 4 shows that the theoretical momentum profiles obtained using the HF method with the aug-cc-pVTZ

basis set (curves 4) can reproduce the experimental data reasonably well, especially in the momentum range below 0.5 a.u. and above 0.8 a.u., and the other calculations with STO-3G, 6-31G and 6-311++G (3df, 3pd) basis sets (curves 1–3) have a relatively higher intensity than the experimental data in the momentum range above 0.8 a.u.. The good performance of the aug-cc-pVTZ basis set indicates that this saturated diffuse and Dunning's correlation consistent polarization basis sets can provide a good prediction of the sulphur-containing five-membered aromatic heterocyclic molecule thiophene.

The experimental and theoretical momentum distributions of the $9a_1$ and $5b_2$ orbitals positioned at 16.6 eV are shown in Fig. 5. The $5b_2$ orbital has a "p-type" character while the $9a_1$ orbital shows an "s-p type" distribution. Then the summed momentum profile is a mixed "s-p type" distribution. The summed theoretical profiles calculated by HF and DFT with aug-cc-pVTZ basis set reproduce the XMP well. A better fit to the XMP by the higher level DFT-B3LYP calculation with aug-cc-pVTZ (curve 7) in the lower momentum region indicates that electron correlation effects are very important for momentum profiles of $9a_1$ and $5b_2$ orbitals. The comparison between the experimental data and theoretical calculations in Fig. 5 shows that all seven calculations somewhat underestimate the experimental intensity in the below 0.2 a.u. momentum region.

The experimental and theoretical momentum profiles for the $8a_1$ orbital are shown in Fig. 6. The TMPs calculated by HF and DFT methods with various basis sets are very similar. Somewhat better fits to the XMPs can be achieved using DFT-B3LYP calculations with aug-cc-pVTZ basis set (curve 7) than the other level calculations with STO-3G, 6-31G and 6-311++G (3df, 3pd) basis sets (curves 1–6) in the momentum region above 0.5 a.u. However, there is a significant discrepancy between all theoretical calculation and experimental data below the momentum of 0.3 a.u., the TMPs underestimate the experimental intensity. The discrepancy between experiment and theory in the low momentum region is probably due to inaccuracies in the Gaussian curve fitting and deconvolution procedures since the nearby two ionization peaks as shown in Fig. 2. In order to further investigate the explanations, the summed experimental data of $9a_1$, $5b_2$ and $8a_1$ orbitals is compared with the summed theoretical ones. The summed TMP gives a very reasonable description for the summed XMP in the lower momentum region. This indicates that the discrepancy between experimental data and theoretical calculations below 0.3 a.u. for the $8a_1$ orbital is mainly due to a possible error in the Gaussian curve fitting and deconvolution procedures.

The IPs of the orbitals $7a_1$ and $4b_2$ are too near to separate entirely. So we give the summed momentum distributions of the $7a_1$ and $4b_2$ orbitals discussed for comparison between experiment and theory. The comparison of the summed XMPs with various calculations in Fig. 7 shows that the theoretical momentum profiles obtained using the HF and DFT-B3LYP methods with all basis sets, except for STO-3G, can reproduce the experimental data reasonably well (curves 2–7).

The experimental and theoretical momentum profiles for the $6a_1$ orbital show strong "s-type" distributions as shown in Fig. 8. All of the TMP curves are multiplied by a factor of 0.60, in order to give a good agreement in shape with the experimental data. The missing intensity (~40%) could be located in higher energy regions of the spectrum. This is supported by the Green's function calculations [9,18]. The calculated momentum profiles from HF and DFT give a similar shape with the XMP.

The peak at ~30.7 eV in the BES (Fig. 2) could be mainly attributed to ionization from the $6a_1$ orbital on the basis of the photon energy dependence of the corresponding photo-ionization cross sections [18]. The presence of a high energy "tail" out to the limit of the data at 35 eV observed in the EMS binding energy spectrum (see Fig. 2) also supports the view that higher energy poles exist. Part of the broadening at high momentum in Figs. 8 and 9 could be due to distortion of the continuum electron waves from plane waves [35]. Generally, higher momentum transfer is contributed from the electron in nearer nucleus region and lower momentum from further nucleus region, so the distortion will become more evident at higher momentum. The quantitative calculation for the distorted wave effects in molecular orbital is still a challenge for theorists so far because of the multi-center systems.

5. Conclusions

In summary, the detailed experimental and theoretical investigations of the valence orbitals electron densities of thiophene by electron momentum spectroscopy are reported. The experimental momentum distributions are compared with the associated calculations with the HF and DFT methods. The binding energies are in excellent agreement with previously published PES data and the synthesized theoretical spectrum are compared with the experimental binding energy spectrum, from which it can be seen that the DFT-B3LYP/aug-cc-pVTZ calculation is in reasonably good agreement with the experimental binding energy spectra in the outer valence region while the calculation predicted significant splitting of ionization transitions from the $6a_1$ inner valence orbital due to strong electron correlation effects in the inner valence region. The agreements between theory and experiment for the shape and intensity of the orbital electron momentum distributions are generally good. HF and DFT calculations with B3LYP hybrid functional using saturated and diffuse basis sets provide some better descriptions of the experimental data. Furthermore in the outer valence orbital momentum distributions the aug-cc-pVTZ calculations give somewhat better fit to the experimental results, which indicates that basis set including saturated diffuse and Dunning's correlation consistent polarization is essential for the sulphur-containing five-membered aromatic heterocyclic

molecule thiophene. The inner valence orbital ionizations are considered with the pole strengths for ionization from these orbitals being split into higher energy satellite processes, which is due to many-body ion states associated with the inner valence orbital ionization.

Acknowledgement

This project received financial support from the National Natural Science Foundation of China under Grant Nos. 19854002, 19774037 and 10274040 and the Research Fund for the Doctoral Program of Higher Education under Grant No. 1999000327. We thank the help of Professor Zhu Qihe.

References

[1] I.E. McCarthy, E. Weigold, Rept. Prog. Phys. 91 (1991) 789, and references therein.
[2] C.E. Brion, Int. J. Quantum Chem. 29 (1986) 1397, and references therein.
[3] C.E. Brion, in: T. Andersen et al. (Eds.), The Physics of Electronic and Atomic Collisions, American Institute of Physics Press, New York, 1993, p. 350.
[4] Y. Zheng, J.J. Neville, C.E. Brion, Y. Wang, E.R. Davidson, Chem. Phys. 188 (1994) 109.
[5] A.D.O. Bawagan, C.E. Brion, Chem. Phys. Lett. 137 (1987) 573.
[6] A.D.O. Bawagan, R. Muller-Fiedler, C.E. Brion, E.R. Davidson, C. Boyle, Chem. Phys. 120 (1988) 335.
[7] E. Weigold, I.E. McCarthy, Electron Momentum Spectroscopy, Kulwer Academic/Plenum Publishers, New York, 1999.
[8] Y. Zheng, W.N. Pang, R.C. Shang, X.J. Chen, C.E. Brion, T.K. Ghanty, E.R. Davidson, J. Chem. Phys. 111 (1999) 9526.
[9] D.M.P. Holland, L. Karlsson, W. von Niessen, J. Electron Spectrosc. Relat. Phenom. 113 (2001) 221.
[10] A.J. Heeger, in: W.R. Salaneck, I. Lundström, B. Rånby (Eds.), Conjugated Polymers, Oxford University Press, New York, 1993.
[11] J.S. Kwiatkowski, J. Leszczyński, I. Teca, J. Mol. Struct. 436–437 (1997) 451.
[12] W. von Niessen, J. Electron Spectrosc. Relat. Phenom. 27 (1989) 129.
[13] T. Munakata, K. Kuchitsu, J. Electron Spectrosc. Relat. Phenom. 20 (1980) 235.
[14] P.J. Derrick, L. Åsbrink, O. Edqvist, B.-Ö. Jonsson, E. Lindholm, Int. J. Mass Spectrom. Ion Phys. 6 (1971) 177.
[15] M.H. Palmer, I.C. Walker, M.F. Guest, Chem. Phys. 241 (1999) 275.
[16] S.A. Chambers, T.D. Tomas, J. Chem. Phys. 67 (1977) 2596.
[17] A. Giertz, M. Bässler, O. Björneholm, H. Wang, R. Feifel, C. Miron, L. Karlsson, S. Svensson, J. Chem. Phys. 117 (2002) 7587.
[18] A.D.O. Bawagan, B.J. Olsson, K.H. Tan, J.M. Chen, B.X. Yang, Chem. Phys. 164 (1992) 283.
[19] M. Takahashi, K. Otsuka, Y. Udagawa, Chem. Phys. 227 (1998) 375.
[20] M. Takahashi, R. Ogino, Y. Udagawa, Chem. Phys. Lett. 288 (1998) 821.
[21] Y. Zheng, C.E. Brion, M.J. Brunger, K. Zhao, A.M. Grisogono, S. Braidwood, E. Weigold, S.J. Chakravorty, E.R. Davidson, A. Sgamellotti, W. von Nessen, Chem. Phys. 212 (1996) 269.
[22] P. Duffy, D.P. Chong, M.E. Cassida, D.R. Salahub, Phys. Rev. A 50 (1994) 4707.
[23] R.D. Nelson Jr., D.R. Lide, A.A. Maryott, Selected values of electric dipole moments for molecules in the gas phase, NSRDS-NBS10, 1967.
[24] P. Duffy, M.E. Casida, C.E. Brion, D.P. Chong, Chem. Phys. 159 (1992) 347.
[25] A.D. Becke, J. Chem. Phys. 98 (1993) 5648.
[26] W.J. Hehre, R.F. Stewart, J.A. Pople, J. Chem. Phys. 51 (1970) 2657.
[27] W.J. Hehre, R. Ditchfield, R.F. Stewart, J.A. Pople, J. Chem. Phys. 52 (1970) 2769.
[28] W.J. Hehre, R. Ditchfield, J.A. Pople, J. Chem. Phys. 56 (1972) 2257.
[29] M.M. Francl, W.J. Petro, W.J. Hehre, J.S. Binkley, M.S. Gordon, D.J. DeFrees, J.A. Pople, J. Chem. Phys. 77 (1982) 3654.
[30] M.J. Frisch, J.A. Pople, J.S. Binkley, J. Chem. Phys. 80 (1984) 3265.
[31] T.H. Dunning Jr., J. Chem. Phys. 90 (1989) 1007.
[32] D.E. Woon, T.H. Dunning Jr., J. Chem. Phys. 98 (1993) 1358.
[33] J.K. Deng, G.Q. Li, Y. He, et al., J. Chem. Phys. 114 (2001) 882.
[34] J.V. Ortiz, V.G. Zakizewski, O. Bolgounircheva, in: J.L. Calais, E. Kryachko (Eds.), Conceptual Perspectives in Quantum Chemistry, Kluwer, New York, 1997, p. 465.
[35] I.E. McCarthy, E. Weigold, Rept. Prog. Phys. 51 (1988) 299.